Journal of Geography and Geology; Vol. 6, No. 2; 2014
ISSN 1916-9779 E-ISSN 1916-9787
Published by Canadian Center of Science and Education

The VISHMOD Methodology with Hydrochemical Modeling in Intermountain (Karstic) Aquifers: Case of the Sierra Madre Oriental, Mexico

Janete Moran-Ramirez[1] & Jose Alfredo Ramos-Leal[2]

[1] Graduate in Applied Geosciences, Institute for Scientific and Technological Research of San Luis Potosi, IPICYT, San Luis Potosi, Mexico

[2] Applied Geoscience Division, Institute for Scientific and Technological Research of San Luis Potosi, IPICYT, San Luis Potosi, Mexico

Correspondence: Jose Alfredo Ramos-Leal, Applied Geoscience Division, IPICYT, San Luis Potosi, Mexico. Tel: 52-444-834-200. E-mail: jalfredo@ipicyt.edu.mx

Received: March 5, 2014 Accepted: April 30, 2014 Online Published: May 7, 2014

doi:10.5539/jgg.v6n2p132 URL: http://dx.doi.org/10.5539/jgg.v6n2p132

Abstract

Hydrogeochemistry can be studied qualitatively using graphics such as scatter plots and Piper, Durov, and Schoeller diagrams, among others, and quantitatively by applying mass balance mixing models. The VISHMOD methodology (Virtual Samples in Hydrochemical Modeling) combines these two forms of hydrogeochemical characterizations. It is performed by applying hydrogeochemical modeling to virtual samples. This method makes standardization and control possible in order to demonstrate the extent to which a model is able to reproduce field measurements. Therefore, hydrogeochemical models of hydrogeological systems must be calibrated. This methodology was applied to carbonate and homogeneous media in the Sierra Madre Oriental in Mexico. Using the VISHMOD methodology in this region resulted in the classification of the water type as calcium bicarbonate (Ca-HCO_3), representing a ternary mixture in which 45.5% was associated with local flow, 38.5% to intermediate flow and 16.5% to water-rock interaction. The main mineral phases were saturated calcite and sub-saturated dolomite, both from limestone contained in the Tamaulipas Formation.

Keywords: end member, groundwater, hydrochemical modeling, ternary mixing, virtual composition, water-rock interaction

1. Introduction

The evolution of groundwater begins when rainwater seeps into the land and is enriched with ions due to interaction with the geological environment during its path. This interaction produces different chemical compositions in the groundwater, based on which different types of groundwater families can be identified.

The evolution of groundwater can be analyzed qualitatively and quantitatively. The former can be accomplished with hydrogeochemical diagrams such as scatter plots, histograms and Piper, Durov, Schoeller, Stiff, Wilcox and Gibbs diagrams. These identify processes such as mixing, ion exchange and water-rock interactions, among others (Gibbs, 1970; Mifflin, 1988; Mazor, 1991; Abu-Jaber, 2001). These models are identified by end members (EM) containing the extreme (maximum and minimum) chemical concentrations in the hydrogeological system. Hydrogeochemical tools such as binary patterns or ternary mixtures are used to quantify these processes (Genereux et al., 1996; Skalbeca et al., 2001; Ramos- Leal et al., 2007; Gómez et al., 2008; Petitta et al., 2010). This identification using EM is based on conservative elements that do not interact with the environment. Chemical reactions are not taken into account by these mixing models.

Another quantitative interpretation tool is hydrogeochemical modeling, in which physical and chemical principles are applied to the simulation of the system. The main objective of modeling is to create or devise theoretical reaction models that can provide elements to explain what is observed in the actual system. These models are constructed using data such as the chemical composition in the aqueous phase, isotope geology and the mineralogy of the system (Hereford et al., 2007; Andre et al., 2004; Lee & Krothe, 2001; Hidalgo et al., 2001). Chemical modeling can be performed in two ways: 1) direct modeling which involves predicting the water composition and the mass transfer that could result from hypothetical reactions and 2) inverse modeling,

which defines mass transfer based on the chemical, mineralogical and isotopic data observed between two points in the system. This paper develops a new methodology, called VISHMOD (Virtual Samples in Hydrochemical Modeling), which unlike other models uses virtual samples constructed from the sum of the mixing fractions of each end member.

The VISHMOD method makes standardization and control possible in order to demonstrate the degree to which a model is able to reproduce field measurements. Therefore, hydrogeochemical models in hydrogeological systems need to be calibrated.

This methodology can be applied to carbonate and homogeneous media. The case study where this method was tested is located in the Sierra Madre Oriental, in Mexico.

2. Method

The details of the sequence of steps taken using the VISHMOD methodology are described below.

(1) Hydrogeochemical Characterization

Chemical data is used to generate Piper diagrams, distribution maps of the hydrogeochemical parameters and Mifflin diagrams to define families, flow systems and geochemical processes. Scatter diagrams are also generated to identify end members and define the type of binary or ternary mixture. The hydrogeochemical characterization provides elements used to build the conceptual model of the hydrogeological system.

(2) Direct Modeling

Groundwater flows through geological material which supplies it with chemical components that form minerals and enrich its composition. To determine whether the precipitation of these minerals is possible, saturation indices (SI = log IAP / K) are obtained through direct modeling with actual data, calculated with the numerical model PHREEQC (Parkhurst & Apello, 1999).

(3) End Member ID (EM)

EM are identified during this stage, which can be based on scatter plots of conservative elements (Cl, Sr, B, Li, Br, F, Ba, isotopes), taking into account the minimum and maximum concentrations in the system. Other cases apply multivariate analysis techniques (Laaksoharju et al., 1999).

(4) Identification of Mixtures

Based on the scatter plot (eg, Cl and Sr) of conservative elements (ie, those that do not chemically react during the evolution of groundwater), three water samples representing the end members (C1, C2 and C3) of a ternary mixture are identified; the remaining are located between the bounds of the mixture lines and are regarded as mixing fractions of the end members. Any water sample from the system can be generated using the three end members.

(5) Mixing Fractions

The chemical composition of each sample (Equation 1) represents the mixing percentage of the three end members in the system.

Where, Cw is the total sum of the three mixing fractions of the EM, obtained using the mass balance equation (Ramos -Leal et al., 2007).

In Equation 1, the total is set equal to 1:

$$Cw = C1 + C2 + C3 = 1 \quad (1)$$

Where, C1 is the EM with lower concentrations in its conservative elements, C2 is the EM with high concentrations in one of the conservative elements; C3 is the EM with the highest concentration of the conservative elements or a high concentration in one of them.

To solve Equation 1 with three unknown variables, a system of 3 equations is needed, for which the concentrations of the conservative elements (eg. C1 and Sr) from the ternary mixture model of the EM are used (Equations 2 and 3).

$$Cw * Clw = C1 * Cl1 + C2 * Cl2 + C3 * Cl3 \quad (2)$$

$$Cw * Srw = C1 * Sr1 + C2 * Sr2 + C3 * Sr3 \quad (3)$$

This results in a system of 3 equations with three unknown variables.

Solving for C1 in Equation 2:

$$C1 = \frac{Cw*Clw - C2*Cl2 - C3*Cl3}{Cl1} \quad (4)$$

Substituting C1 in Equation 1:

$$Cw = \frac{Cw*Clw - C2*Cl2 - C3*Cl3}{Cl1} + C2 + C3 \quad (5)$$

Solving C3 and simplifying:

$$C3 = \frac{Cw(Cl1 - Clw) + C2(Cl2 - Cl1)}{Cl1 - Cl3} \quad (6)$$

In Equation 3 we solve for C3:

$$C3 = \frac{Cw*Srw - C1*Sr - C2*Sr2}{Sr3} \quad (7)$$

Substituting the value of C3 in Equation 1 and simplifying:

$$Cw = \frac{C1(Sr3 - Sr1) + C2(Sr3 - Sr2) + CwSrw}{Sr3} \quad (8)$$

Solving for C1 and simplifying:

$$C1 = \frac{Cw(Sr3 - Srw) + C2(Sr2 - Sr3)}{(Sr3 - Sr1)} \quad (9)$$

The EMs are calculated using Equation 6 for C3 and Equation 9 for C1.

The only solution for C2 when CW = 1 can be obtained by substituting C1 and C3 in Equation 1:

$$C2 = 1 - C1 - C3 \quad (10)$$

(6) Resulting Virtual Samples

Based on the mixing fraction of each of the end members, the chemical composition of each sample in the system is obtained; this resulting composition represents a virtual chemical composition that does not consider the water-rock interaction. It is used in the process to chemically model system.

(7) First Calibration (actual versus virtual chemical composition data 1)

Calibration can be performed qualitatively and quantitatively. The former can be conducted using hydrogeochemical diagrams such as Durov, Piper and Stiff, among others. Piper diagrams are used by the methodology presented herein, with which the modeled results are compared to the actual data corresponding to the different stages. The quantitative calibration of the model with actual data is performed by obtaining an ionic delta, which is the difference between its parameters. This enables us to observe whether there are differences between the virtual chemical compositions and the actual data. In particular cases, the ionic delta can be close to zero, indicating that mixing is the dominant process in the chemical evolution of groundwater in the system. Inverse modeling or water-rock interactions are not needed for these cases.

(8) Modeling with Water-Rock Interaction

Taking into account the saturation indices (SI) obtained from the actual data and that the mineral phases are consistent with the geology of the hydrogeological system, the rock-water interaction is modeled with the data from virtual composition 1 obtained from the mixing model. Using this modeling, virtual composition 2 is obtained, which considers the interaction with the major minerals. The stability of the mineral phases depends on the physicochemical conditions of the system, for which phase diagrams are used.

(9) Second Calibration (actual versus virtual chemical composition data 2)

The Piper diagram is used again to compare actual data to virtual chemical composition 2. If an ion delta exists, that would be indicative of other processes occurring, such as ion exchange, dissolution and/or precipitation of the main mineral phases. In these cases, inverse modeling is applied as a next step to identify and quantify these processes. If the ionic delta is close to zero, this would indicate that the mixing and the water-rock interaction were the dominant processes in the system. And lastly, calibration is performed.

3. Results

3.1 Case Study

The VISHMOD methodology was applied to the Sierra Madre Oriental (SMO) in eastern Mexico. The hydrogeochemical data were obtained in March 2010 with 24 samples from springs and wells in the valley of San Felipe Orizatlan (VSFO) (Figure 1, Table 1). All samples were collected in 60 ml polyethylene (HDLP)

bottles. For anions, the bottles were washed and rinsed seven times with deionized water, while for cations and trace elements they were washed with 10% HCl and then rinsed seven times with deionized water.

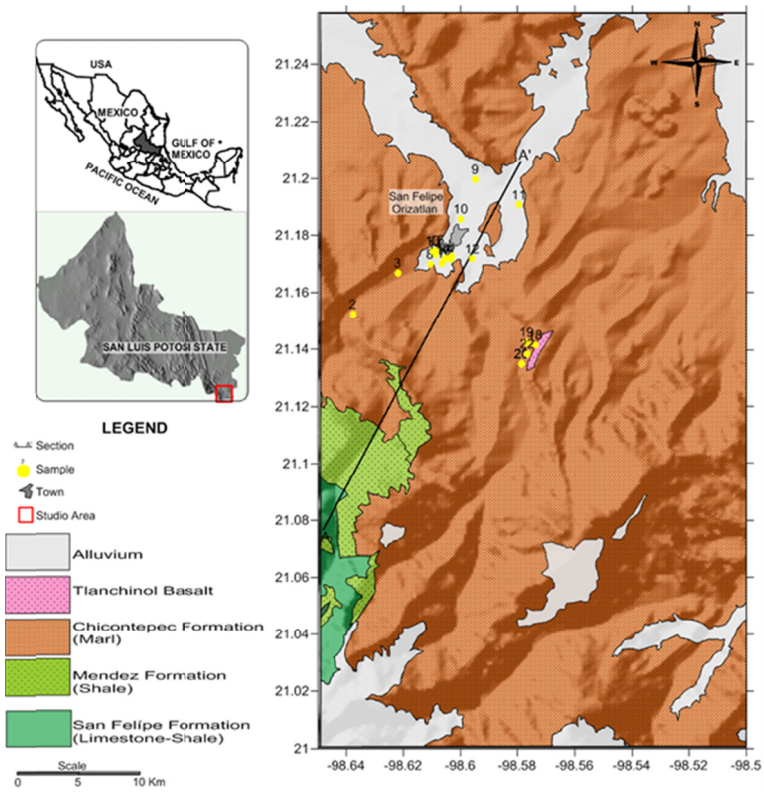

Figure 1. Location and geology of the study area

For cations and trace elements, after the sample was obtained, it was acidified with concentrated HNO_3 to reach a pH <2. Anion samples were not acidified. All samples were stored at a temperature under 4 °C. For each sample, the following was measured in situ: pH, total electrical conductivity, alkalinity by titration, oxide reduction potential (ORP), dissolved oxygen (DO), total dissolved solids (TDS) and temperature. The major ions and trace elements were sent to the Geosciences Laboratory of the National Autonomous University of Mexico where they were analyzed using Inductively Coupled Plasma - Optical Emission Spectrometry, Thermo Model ICAP 6500Duo. The anions (SO_4 and Cl) were analyzed with colorimetry at the Potosino Institute for Scientific and Technological Research. The ionic balance of the chemical data had an error of less than 10%.

a) Geology

The springs are located in the marl Chicontepec Formation and the wells in the alluvium. The subsoil consists of sedimentary rocks ranging in age from Mesozoic to Recent (Figures 1 and 2). The oldest rocks are Lower Cretaceous (Cenomanian-Berrasian) from the undifferentiated Tamaulipas Formation, which consists of a sequence of limestone and shale. Above this is the Agua Nueva Formation, a transitional layer consisting of a limestone-clay sequence from the Cenomanian-Turonian age. The San Felipe Formation was deposited on top (transitional and evenly) which contains a sequence of calcareous marl with interbedded shale from the Coniacian-Santonian age. Uneven sandy-clay rocks from the Paleocene-Eocene age are found above in the Chicontepec Formation. These rock outcroppings are present throughout most of the area, forming an irregular alternation of sandstone and shale whose thickness varies at times. Miocene volcanic rocks are present, characterized by small basaltic and andesitic flows, identified as Tlanchinol Basalt. Lastly, deposits from the Holocene age are found covering Tertiary sediments, made up of round and partially round fragments of different grain sizes such as sand, gravel, clay and silt deposited in rivers and streams by water courses and transported to and deposited in meanderings and floodplains; these deposits unevenly cover all the units described above.

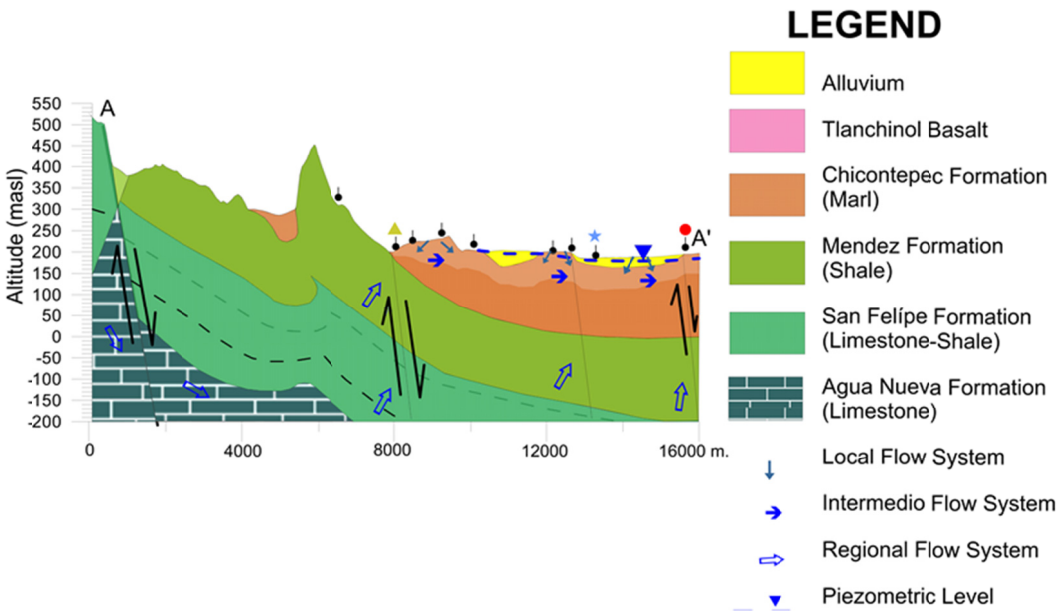

Figure 2. Model hydrogeological section conceptual

b) Hydrogeology

The hydrogeological system is composed of 6 units grouped into aquifers (Agua Nueva F., Chicontepec F., Alluvium and basalts) and aquitards (San Felipe F. and Méndez F.). Figure 2 represents a SW-NE section showing the layout of the Cretaceous and Tertiary formations, synclinal valleys and anticlinal mountains.

The main recharge area is located in the highlands of the SMO in the western portion of the study area (C1), where exposed Cretaceous rocks are found, such as those of the Agua Nueva Formation (Figure 2). The infiltrating water is confined by argillaceous limestone from the San Felipe Formation and shale from the Mendez Formation (C2). Nevertheless, the presence of normal faults facilitates the upward vertical flow in end member 3 (C3), producing the springs in the study area (Figure 2). The flow direction is mainly from west to east (Figure 2). The marl belonging to the Chicontepec Formation is located on top of the aquitards in the San Felipe and Mendez Formations, through which the water from end member 2 (C2) flows (intermediate flow) from west to east (Figure 2). Alluvial deposits made up of gravel and sand that capture the local flow (C1) are found on top.

The presence of faults and fractures that cut through the SMO bends provide the hydraulic connection that results in regional flows (C3) mixing with shallow flows C1 and C2 (Figure 2).

c) Results and Discussion

The Mifflin diagram, which compares Na + K vs Cl+SO_4, identifies three main flow systems: a local system with a low content of these components, an intermediate with the highest concentration and a system of regional flow with high Na+K and SO_4+Cl values (Figure 3).

The recharge area of the system, is located in the mountainous area to the SW of the study area, which is characterized by low temperatures (< 21 °C) Electrical Conductivity less than 400 µS/cm and Chlorides with lower values 2 mg/L (Fig.4).

The discharge area is located to the north, is identified as having high temperatures (> 25 °C), CE greater than 900 µS/cm and concentrations greater than 18 mg/L of chloride (Figure 4).

Groundwater flow is from the higher areas of the SW to the valleys in the NE (Figures 1 and 3). This coincides with the distribution of samples in Mifflin diagrams and ternary mixture model, where the samples near the origin are in the recharge area and the most evolved or regional flow toward the other extreme (Figures 1, 2, 3).

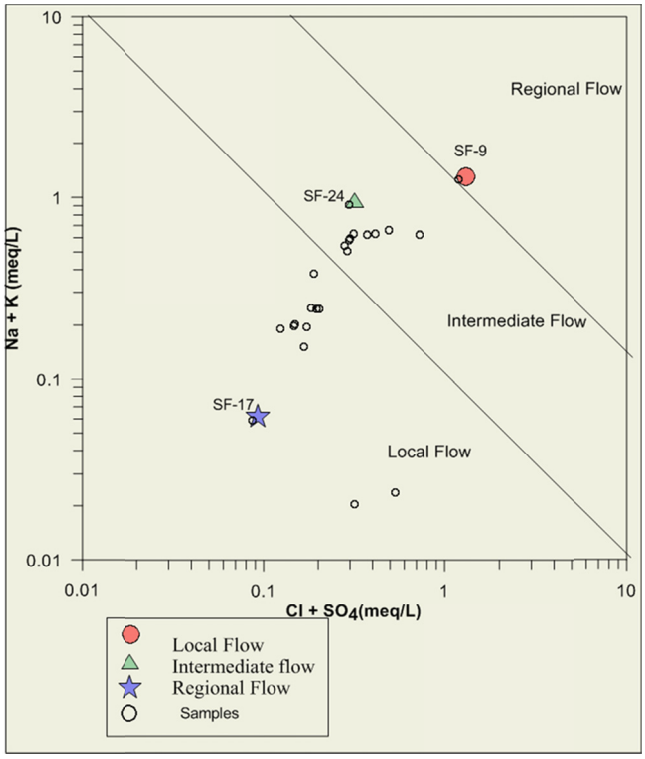

Figure 3. Mifflin diagram, flow identification systems

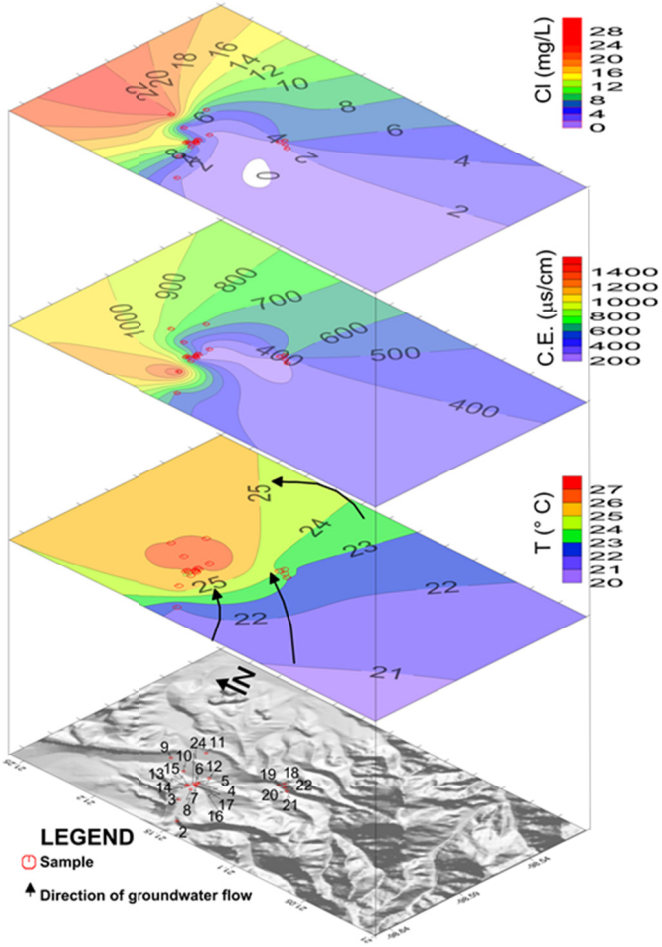

Figure 4. Distribution of chloride, temperature and electrical conductivity in the study area

The Piper diagram presented in Figure 5 shows a calcium bicarbonate water family (Ca-HCO_3-). This family is produced by the movement of groundwater through limestone, which dissolves the carbonate rock as it flows due to the water-rock interaction.

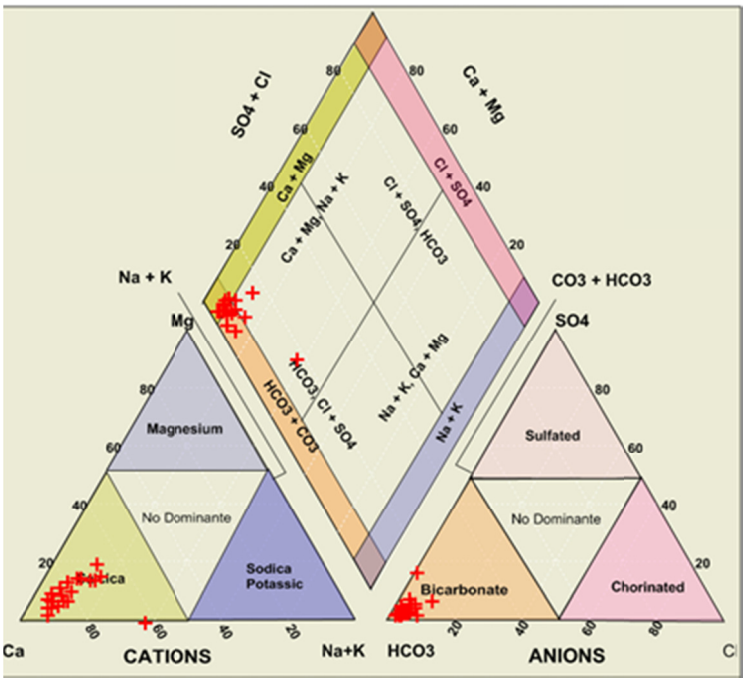

Figure 5. Piper Diagram of Water Sampled in the Intermountain VSFO valleys

The scatter plot of Cl and Sr also identifies three end members (C1, C2, C3), indicating the different sources of input into the system. Each supply source has a different evolution (Figure 6).

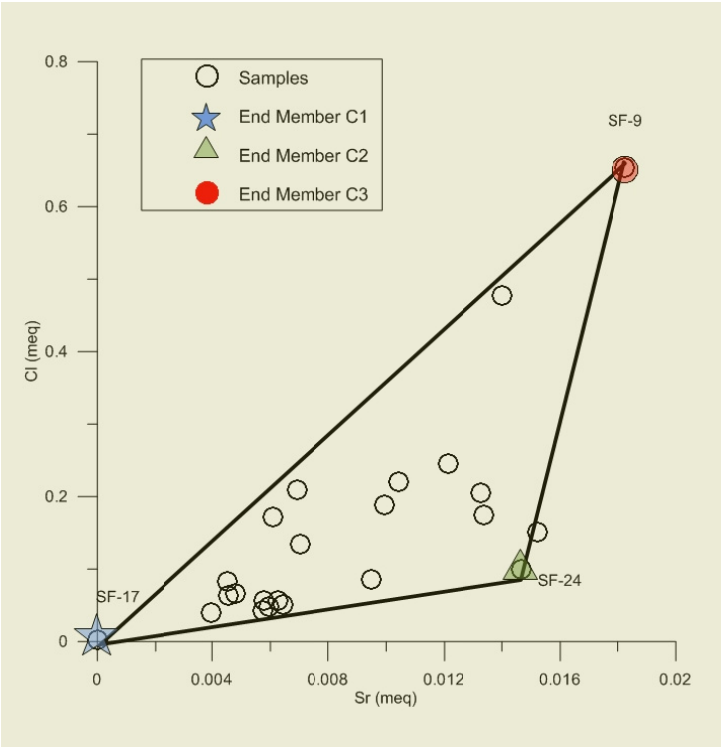

Figure 6. Ternary mixture model using Cl and Sr concentrations, in the inter-mountain valley where C1, C2 and C3 are end members

Table 1. Physicochemical data samples from the VSFO (meq/L)

Sample	X	Y	Temp °C	pH	Eh mV	Cond MS/cm	Alkalinity meq/L	Cl meq/L	SO_4 meq/L	Ca meq/L	K meq/L	Mg meq/L	Na meq/L	Sr meq/L
SF-01	534484	2334053	21	7.3	0.83		2.623	0.063	0.104	2.350	0.021	0.167	0.130	0.005
SF-02	537515	2339032	22	7.3	0.45	580	2.951	0.066	0.083	2.700	0.069	0.167	0.130	0.005
SF-03	539166	2340663	26	6.8	94	1440	5.459	0.174	0.125	6.500	0.033	0.750	0.565	0.013
SF-04	541137	2341192	26	7	80	420	3.689	0.209	0.208	3.450	0.159	0.667	0.478	0.007
SF-05	541165	2341337	26	7.2	83	470	4.262	0.134	0.146	4.500	0.154	0.333	0.391	0.007
SF-06	540945	2341248	26	7.1	81	430	3.689	0.171	0.125	4.050	0.192	0.417	0.391	0.006
SF-07	540814	2341042	26	7.3	59	300	2.459	0.083	0.208	2.300	0.121	0.500	0.391	0.005
SF-08	540369	2341013	25	7.1	74	610	5.656	0.189	0.125	3.400	0.110	0.750	0.522	0.010
SF-09	542027	2344338	26	6.9	106	840	5.902	0.654	0.542	6.450	0.041	1.917	1.217	0.018
SF-10	541501	2342776	27	6.9	100	530	4.426	0.086	0.104	5.200	0.036	0.667	0.348	0.010
SF-12	543662	2343331	26	6.9	105	680	6.492	0.206	0.167	6.650	0.021	0.583	0.609	0.013
SF-13	541923	2341218	27	8.1	50	280	2.459	0.057	0.125	2.650	0.031	0.417	0.217	0.006
SF-14	540470	2341530	25	6.8	98	740	5.902	0.477	0.250	6.850	0.021	0.833	0.609	0.014
SF-15	540563	2341396	24	7.3	0.3	360	3.000	0.043	0.104	3.650	0.023	0.250	0.174	0.006
SF-16	540620	2341553	26	6.8	110	720	5.902	0.246	0.250	6.800	0.054	0.667	0.609	0.012
SF-17	540867	2341171	22	6.6	147	20	0.393	0.003	0.083	0.100	0.015	0.000	0.043	0.000
SF-18	540863	2341179	25	7	74	710	6.590	0.151	0.167	6.200	0.023	1.333	0.826	0.015
SF-19	544273	2337829	23	6.8	73	650	5.311	0.220	0.313	6.900	0.021	0.500	0.478	0.010
SF-20	543958	2337927	24	7.2	92	340	3.049	0.057	0.146	3.350	0.026	0.417	0.217	0.006
SF-21	543762	2337093	23	7.1	79	290	2.754	0.049	0.125	3.050	0.021	0.417	0.174	0.006
SF-22	543762	2337093	21	8	18	190	1.967	0.040	0.083	1.650	0.015	0.333	0.174	0.004
SF-23	543977	2337480	24	6.8	103	350	3.197	0.051	0.146	3.400	0.026	0.417	0.217	0.006
SF-24	541501	2343331	24.6	7.1	74	521.5	7.086	0.100	0.179	6.665	0.025	1.433	0.887	0.015

C1 is associated with local recharge and is located in the central part of the VSFO in the valley's alluvial materials. Cl and Sr were low and the temperature was 22 °C. The lowest values (Cl of 0.0045 meq/L and Sr less than 0.01 meq /L) were found in sample 17 (Figures 2, 3 and 6).

C2 is represented by sample 24 and is located in the northern part of valley. It is associated with intermediate flow, had a temperature of 24.6 °C, concentrations of Cl (0.099 meq/L) and a high concentration of Sr (0.0146 meq/L) (Figures 2, 3 and 6).

C3 is represented by Sample 9, located in the limestone found in the region. It is associated with regional flow from the SMO. Sample 9 is the most representative of this member, and had a temperature of 26 °C, Cl concentrations of 0.654 meq/L and Sr of 0.0182 meq/L (Figures 2, 3 and 6). By applying the ternary mixture model, the percentages supplied by each flow system represented by the end members were obtained (Table 2).

According to the ternary mixture model for the water in the study area, C1 (local recharge) is associated with 45.5%, C2 (intermediate flow) with 38.5% and C3 (regional flow) 16% (Table 2). Mostly binary mixtures were identified in samples 15, 18, 21, 23.

The virtual chemical composition of the water samples (Table 3) was obtained based on the mixing fractions. The Piper diagram (Figure 7) shows a difference between the virtual chemical composition and the actual data from the water in the study area. This difference is largely because up to this point the virtual composition was not considered in the water-rock interaction process.

In response to the above, the actual samples were directly modeled to obtain the mineral phases present in groundwater (Figure 8), which were used for the water-rock interaction in the virtual composition samples (Table 3) in order to identify the hydrogeochemical processes involved in the actual chemical composition.

Table 2. Mixing fractions for groundwater from the VSFO

Station ID	C1	C2	C3	CT
SF-01	0.7	0.25	0.05	1
SF-02	0.68	0.27	0.05	1
SF-03	0.12	0.75	0.13	1
SF-04	0.6	0.1	0.3	1
SF-05	0.56	0.29	0.15	1
SF-06	0.64	0.12	0.24	1
SF-07	0.71	0.2	0.09	1
SF-08	0.37	0.42	0.21	1
SF-09	0	0	1	1
SF-10	0.35	0.63	0.02	1
SF-12	0.14	0.67	0.19	1
SF-13	0.61	0.37	0.02	1
SF-14	0.22	0.06	0.72	1
SF-15	0.6	0.4	0	1
SF-16	0.24	0.47	0.29	1
SF-17	1	0	0	1
SF-18	0	0.94	0.06	1
SF-19	0.35	0.38	0.27	1
SF-20	0.58	0.41	0.01	1
SF-21	0.59	0.41	0	1
SF-22	0.73	0.26	0.01	1
SF-23	0.55	0.45	0	1
SF-24	0	1	0	1

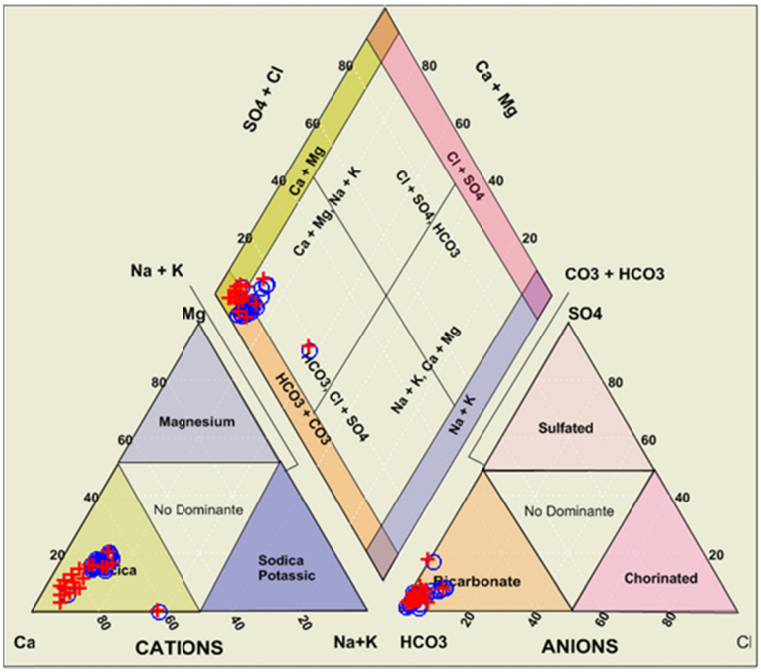

Figure 7. Piper diagram representing the difference between the actual mixtures and the mixing model (O represents the theoretical samples, + represents the actual samples)

Table 3. Virtual chemical composition 1, of the mixture

Station ID	X	Y	Temp	pH	HCO_3	Cl	SO_4	Na	Ca	K	Mg
SF-01	534484	2334053	21	7.3	2.349	0.062	0.129	0.312	2.063	0.0189	0.43
SF-02	537515	2339032	22	7.3	2.447	0.0657	0.131	0.326	2.161	0.0191	0.47
SF-03	539166	2340663	26	6.8	6.14	0.174	0.215	0.83	5.862	0.0258	1.31
SF-04	541137	2341192	26	7	2.721	0.208	0.229	0.479	2.665	0.0239	0.709
SF-05	541165	2341337	26	7.2	3.179	0.134	0.18	0.466	2.975	0.0219	0.698
SF-06	540945	2341248	26	7.1	2.518	0.171	0.204	0.426	2.411	0.0226	0.624
SF-07	540814	2341042	26	7.3	2.212	0.082	0.142	0.314	1.967	0.0195	0.448
SF-08	540369	2341013	25	7.1	4.345	0.188	0.22	0.643	4.178	0.0247	0.99
SF-09	542027	2344338	26	6.9	5.89	0.654	0.541	1.216	6.443	0.041	1.891
SF-10	541501	2342776	27	6.9	4.693	0.085	0.151	0.593	4.334	0.0217	0.921
SF-12	543662	2343331	26	6.9	5.921	0.205	0.236	0.833	5.707	0.0266	1.31
SF-13	541923	2341218	27	8.1	2.979	0.057	0.127	0.379	2.656	0.0193	0.561
SF-14	540470	2341530	25	6.8	4.758	0.477	0.417	0.937	5.06	0.0343	1.445
SF-15	540563	2341396	24	7.3	2.735	0.042	0.116	0.338	2.398	0.0186	0.495
SF-16	540620	2341553	26	6.8	5.183	0.245	0.261	0.78	5.027	0.0272	1.214
SF-17	540867	2341171	22	6.6	0.393	0.0028	0.083	0.043	0.1	0.0153	0
SF-18	540863	2341179	25	7	7.05	0.15	0.202	0.915	6.72	0.026	1.458
SF-19	544273	2337829	23	6.8	4.407	0.22	0.243	0.478	6.9	0.0205	0.493
SF-20	543958	2337927	24	7.2	3.225	0.057	0.127	0.405	2.888	0.0195	0.606
SF-21	543762	2337093	23	7.1	3.07	0.048	0.121	0.379	2.715	0.0191	0.563
SF-22	543762	2337093	21	8	2.108	0.04	0.106	0.259	1.786	0.0176	0.363
SF-23	543977	2337480	24	6.8	3.07	0.051	0.121	0.38	2.726	0.0191	0.566
SF-24	541501	2343331	24.6	7.1	7.086	0.117	0.179	0.886	6.666	0.0248	1.415

The resulting hydrogeochemical model is an approach to the actual processes occurring in the aquifer and reflects interaction with carbonate rocks in the region. This suggests interaction with rocks composed of limestone from the undifferentiated Tamaulipas Formation, marl from the San Felipe Formation and shale from the Chicontepec Formation, since the most important mineral phases are calcite and dolomite. The calcite in the study area is slightly saturated, while gypsum and dolomite are under-saturated, indicating a dissolution of these minerals from contact with the water as it passes through these rocks. In some cases, the dolomite may be saturated due to the presence of Mg. Celestite is under-saturated in all samples. Barite is very close to equilibrium and, therefore, it is sometimes under-saturated or saturated (Table 4 and Figure 8).

As shown by the Piper diagram (Figure 9), the chemical composition obtained by the virtual mixing modeled with rock-water interaction fits the actual samples, indicating that the main process occurring in the system are the mixture with water-rock interaction (Table 4).

Table 4. Virtual chemical composition 2, of the mixture without water-rock interaction

Station ID	X	Y	Temp	pH	HCO3	Cl	SO4	Na	Ca	K	Mg
SF-01	534484	2334053	21	7.3	2.9	0.062	0.11	0.29	2.2	0.02	0.2
SF-02	537515	2339032	22	7.3	3.2	0.0657	0.1	0.3	2.5	0.07	0.2
SF-03	539166	2340663	26	6.8	6	0.174	0.13	0.6	6	0.03	0.65
SF-04	541137	2341192	26	7	4	0.208	0.21	0.5	3	0.16	0.7
SF-05	541165	2341337	26	7.2	4	0.134	0.15	0.46	4	0.15	0.34
SF-06	540945	2341248	26	7.1	4	0.171	0.13	0.42	4.4	0.22	0.32
SF-07	540814	2341042	26	7.3	2.5	0.082	0.21	0.38	2	0.02	0.45
SF-08	540369	2341013	25	7.1	6	0.188	0.13	0.5	4	0.12	0.99
SF-09	542027	2344338	26	6.9	5.9	0.654	0.54	1.21	6.44	0.041	1.89
SF-10	541501	2342776	27	6.9	4.6	0.085	0.11	0.4	4.9	0.03	0.92
SF-12	543662	2343331	26	6.9	6	0.205	0.18	0.7	6.5	0.026	0.6
SF-13	541923	2341218	27	8.1	3	0.057	0.13	0.3	2.6566	0.029	0.55
SF-14	540470	2341530	25	6.8	6	0.477	0.3	0.65	7	0.03	0.72
SF-15	540563	2341396	24	7.3	3	0.042	0.11	0.2	4	0.02	0.245
SF-16	540620	2341553	26	6.8	6	0.245	0.26	0.63	7	0.03	0.6
SF-17	540867	2341171	22	6.6	0.4	0.0028	0.0833	0.0434	0.1	0.015	0
SF-18	540863	2341179	25	7	6.8	0.15	0.17	0.03	0.3	0.001	0.7
SF-19	544273	2337829	23	6.8	5.5	0.22	0.3	0.03	0.4	0.01	0.012
SF-20	543958	2337927	24	7.2	3.2	0.057	0.145	0.2	3	0.02	0.6
SF-21	543762	2337093	23	7.1	3	0.048	0.13	0.2	2.8	0.02	0.56
SF-22	543762	2337093	21	8	2	0.04	0.09	0.2	1.8	0.016	0.36
SF-23	543977	2337480	24	6.8	3	0.051	0.15	0.2	3	0.02	0.56
SF-24	541501	2343331	24.6	7.1	7.086	0.117	0.18	0.9	6.66	0.024	1.415

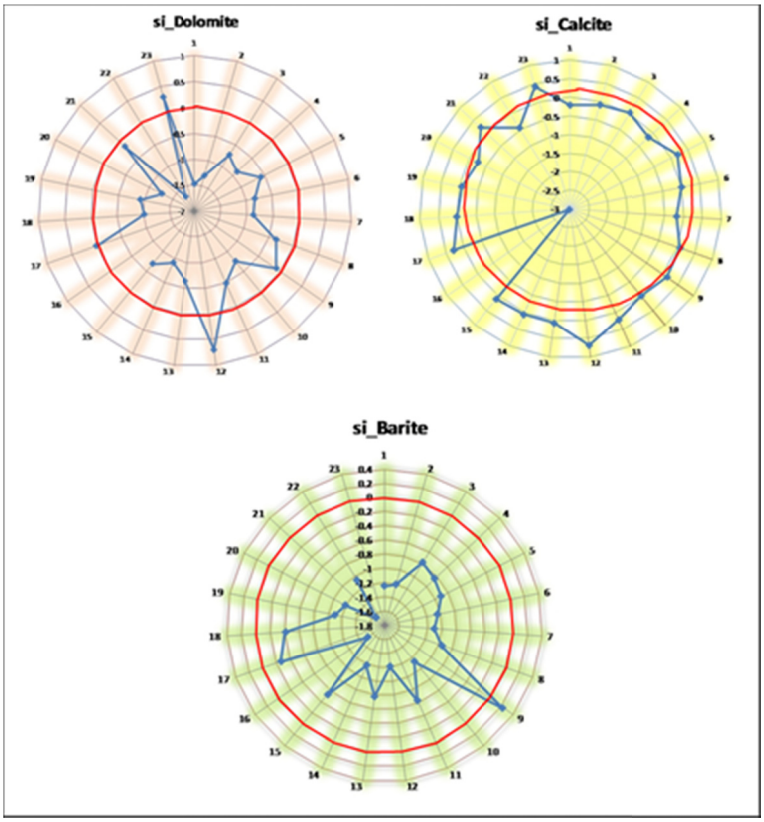

Figure 8. Saturation indices for Dolomite, Calcite and Barite

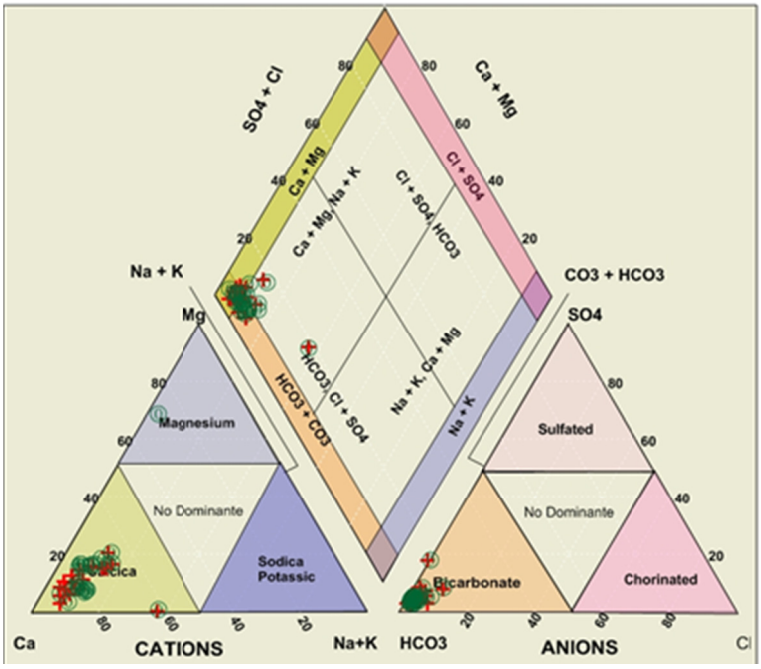

Figure 9. Field Samples with Synthetic Model 2, applying the water-rock interaction (O represents the theoretical samples, + represents the actual samples)

4. Conclusions

The Sierra Madre Oriental has a regional recharge area, an intermediate area in the mountainous Sierra Madre Oriental and local recharge in the intermountain valleys in the region.

The main groundwater family in the intermountain valleys of the VSFO is calcium bicarbonate (Ca-HCO_3).

Water from the VSFO aquifer represents the ternary mixture of three end members that correspond to local flow (C1), representing 45.5%, intermediate flow (C2) representing 38.5% and regional flow (C3) representing 16.5%.

The mixture model provides the first approach to analyzing the virtual chemical composition of groundwater, although the chemical differences between the virtual composition and the actual data indicate that other physical and chemical processes occur, such as water-rock interactions, dissolution and precipitation of minerals.

Modeling of the chemical composition with water-rock interactions notably reduced the chemical differences.

The main processes identified by the application of the VISHMOD were ternary mixture and rock-water interactions which involved the precipitation of calcite and the dissolution of dolomite.

The results from the application of the VISHMOD methodology demonstrate that it is an effective tool to identify and simulate mixing processes involving water-rock interactions and the precipitation and dissolution of minerals occurring in carbonate aquifers in the region.

References

Abu-Jaber, N. (2001). Geochemical evolution and recharge of the shallow aquifers at Tulul al Ashiqif NE. *Jordan: Environ. Geol., 41*, 372-383. http://dx.doi.org/10.1007/s002540100402

Apello, C. A., & Postma, D. (1996). *Geochemistry, groundwater and pollution: A. A. Balkema, Rotterdam* (p. 536).

André, M., Franceschi, P., Pouchan, O., & Atteia. (2004). Using geochemical data and modelling to enchance the understanding of groundwater flow in a regional deep aquifer, Aquitaine Basin. *Journal of Hydrology, 305*, 40-60. http://dx.doi.org/10.1016/j.jhydrol.2004.08.027

Genereux, D., Wood, S. J., & Pringle, C. M. (1996). Chemical mixing model of streamflow generation at La Selva Biological Station, Costa Rica. *Journal of Hidrology, 199*, 319-330. http://dx.doi.org/10.1016/S0022-1694(96)03333-1

Gibbs, R. J. (1970). Mechanisms Controlling World Water Chemistry. *Science, 170*(3962), 1088-1090. http://dx.doi.org/10.1126/science.170.3962.1088

Gómez, J. B., Aunqué, L. F., & Gimeno, M. J. (2008). Sensivity and uncertainty analysis of mixing and mass balance calculations whit Standard and PCA-based geochemical codes. *Applied Geochemistry, 23*, 1941-1956. http://dx.doi.org/10.1016/j.apgeochem.2008.02.019

Hereford, G., Keating, H., Guthrie, Jr. D., & Chen, Z. (2007). Reactions and reaction rates in the regional aquifer beneath the Pajarito Plateau, north-central New Mexico: USA. *Environ. Geol., 52*, 965-977. http://dx.doi.org/10.1007/s00254-006-0539-z

Hidalgo, M. C., & Cruz-Sanjulián, J. (2001). Groundwater composition, hydrochemical evolution and mass transfer in a regional detrital aquifer (Baza Basin, Southern Spain). *Applied Geochemistry, 16*(7), 745-758. http://dx.doi.org/10.1016/S0883-2927(00)00078-0

Laaksoharju, M., Skarman, C., & Skarman, E. (1999). Multivariate Mixing and mass balance (M3) calculation a new tool for decuding hydrogeochemical information. *Applied Geochemistry, 14*, 861-871. http://dx.doi.org/10.1016/S0883-2927(99)00024-4

Lee, E. S., & Krothe, N. C. (2001). A four-component mixing model for water in a karst terrain in south-central Indiana, USA. Using solute concentration and stable isotopes as tracers. *Chem. Geol., 179*, 129-143. http://dx.doi.org/10.1016/S0009-2541(01)00319-9

Mazor, E. (1991). *Chemical and isotopic groundwater hydrology the applied approach* (p. 412).

Mifflin, M. D. (1988). Region 5, Great Basin. In W. Back, J. S. Rosenshein & P. R. Seaber (Eds.), *Hydrogeology, Geological Society of America* (pp.69-78).

Parkhurst, D. L., & Appelo, C. A. J. (1999). User's guide to PHREEQC (Version 2): A computer program for speciation, batch-reaction, one-dimensional transport, and inverse geochemical calculations. *U. S. Geological Survey Water Resources Investigations Report*.

Petitta, M., Primavera, P., Tuccimei, P., & Aravena, R. (2011). Interaction between deep and shallow groundwater systems in areas affected by Quaternary tectonics (Central Italy): a geochemical and isotope approach. *Environmental Earth Sciences, 63*(1), 11-30. http://dx.doi.org/10.1007/s12665-010-0663-7

Ramos-Leal, J. A., Martínez-Ruiz, V. J., Rangel-Mendez, J. R., & de la Torre, M. A. (2007). Hydrogeological and mixing process of waters in aquifers in arid regions: a case study in San Luis Potosi Valley, Mexico. *Environmental geology, 53*(2), 325-337. http://dx.doi.org/10.1007/s00254-007-0648-3

Skalbeck, J. D., Shevenell, L., & Widmer, C. M. (2001). Mixing of termal and non-thermal waters in the Steamboat Hills area, Nevada, USA. *Geothermics, 31*, 69-90. http://dx.doi.org/10.1016/S0375-6505(01)00010-4